



Effects of self-erasing discharge on panel-aging characteristics in AC plasma display panel

Choon-Sang Park^a, Heung-Sik Tae^{a,*}, Eun-Young Jung^b, Jeong-Chull Ahn^c

^a School of Electrical Engineering and Computer Science, Kyungpook National University, Daegu, Republic of Korea

^b Core Technology, Corporate R&D Center, Samsung SDI Company Ltd., Youngin, Republic of Korea

^c Advanced Development TF, PDP Division, Samsung SDI Company Ltd., Youngin, Republic of Korea

ARTICLE INFO

Available online 16 May 2010

Keywords:

Surface morphology
MgO thin film
Self-erasing discharge
Panel-aging
Three-dimensional IR emission
Wall charge distribution
Electric field strength
Impulse

ABSTRACT

This paper investigates the changes in the surface morphology of the MgO thin film on the ITO and bus electrodes in ac plasma display panel under various sustain voltages during the panel-aging process. It is found that the achievement in the stable discharge in an AC-PDP by means of the panel-aging process strongly depends on whether the surface morphologies of the MgO thin film are identical on both the ITO and bus electrodes. It is also found that the self-erasing discharge during the panel-aging process is not effective in obtaining the uniform surface morphology of the MgO thin film on the ITO and bus electrodes, due to the difference in the amount of ion bombardment on the ITO and bus electrodes caused by the erasing of the wall charges during the self-erasing discharge. These experimental results are confirmed by monitoring the three-dimensional IR emission and simulating the wall charge distribution, the electric field strength, and the impulse on the MgO layer.

© 2010 Elsevier B.V. All rights reserved.

1. Introduction

The MgO layers have been used as a protective layer in AC-PDPs due to their high stability against ion bombardment, low optical loss, high thermal stability, and good electrical insulating properties. The initial surface states of the MgO thin film prepared by the ion-plating method are very non-uniform. Accordingly, the panel-aging process is necessary to obtain the uniform MgO surface condition for the stable discharge [1–5]. As such, the surface condition of the MgO layer after the panel-aging process plays a decisive role in determining the initial discharge characteristics in an AC-PDP panel [5–8]. Recently, to lower the panel fabrication cost, the PDP industry is focused on reducing the panel-aging process time. One of the methods to reduce the panel-aging process time is simply to use the higher sustain voltage during the panel-aging process. However, our experimental results show that the use of the higher sustain voltage during the panel-aging process results in the unstable discharge. In the case of the higher sustain voltage, we have observed the different surface morphologies of the MgO thin film on the ITO and bus electrodes.

Accordingly, this paper examines the changes in the surface morphology of the MgO thin film on the ITO and bus electrodes relative to the sustain voltage level during the panel-aging process by monitoring the three-dimensional IR emission and simulating the wall charge distribution, the electric field strength, and the impulse on the MgO layer. The used test panels are a 42-in. AC-PDP and 2-in. test panel with an He (35%)–Xe (11%)–Ne gas compositions and box-type barrier. In particular, 2-in. test panel is fabricated to measure the 3-dimensional IR emission using the ICCD.

2. Experimental setup

Fig. 1 shows the optical-measurement systems and 42-in. and 2-in. test panels with three electrodes, where X is the sustain-, Y the scan-, and A the address-electrode. A pattern generator, signal generator, ICCD camera, and photo-sensor amplifier (Hamamatsu, C6386) were used to measure the IR emission and ICCD image, respectively. Fig. 2 shows the single pixel structure of the 42-in. HD AC-PDP panel employed in this research. The indium tin oxide (ITO) electrode has a low conductivity, whereas the bus electrode made from Silver has a high conductivity. The gap between the two ITO electrodes is short, whereas the gap between the bus electrodes is long. The detailed panel specifications are listed in Table 1.

In this experiment, a 2-in. test panel was specially fabricated without phosphor layer only to investigate the three-dimensional IR

* Corresponding author. School of Electrical Engineering and Computer Science, Kyungpook National University, E10-911, 1370 Sangyuk-dong, Buk-gu, Daegu 702-701, Republic of Korea. Tel.: +82 53 950 6563; fax: +82 53 950 5505.

E-mail address: hstae@ee.knu.ac.kr (H.-S. Tae).

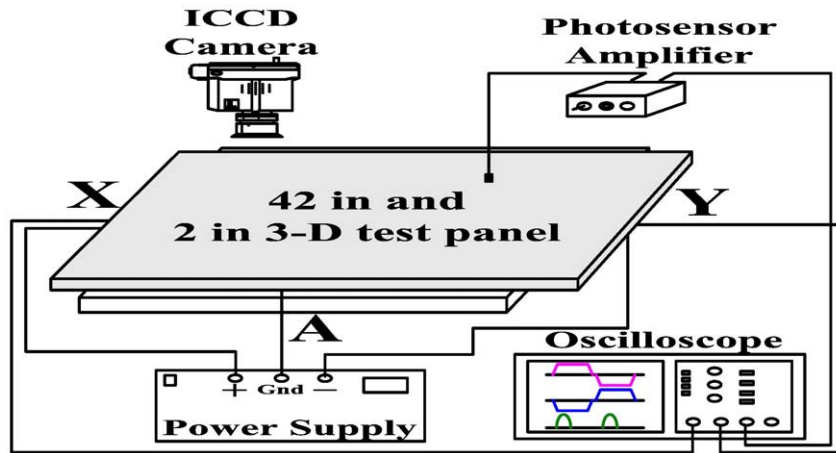


Fig. 1. Schematic diagram of experimental setup employed in this research.

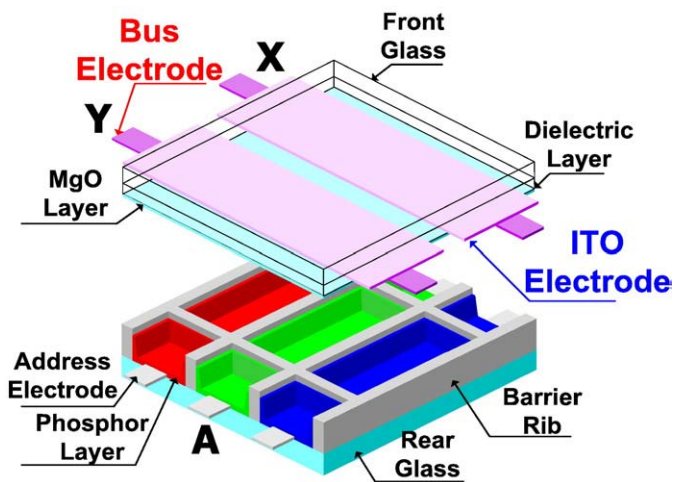


Fig. 2. Schematic diagram of single pixel structure in 42-in. HD AC-PDP.

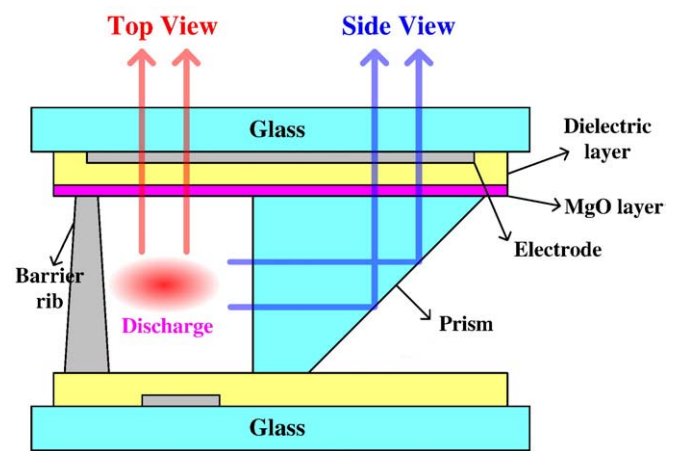


Fig. 3. Schematic diagram of single pixel structure in 2-in. test panel having exactly same structure as 42-in. AC-PDP.

emission during the plasma discharge in AC-PDP. Fig. 3 shows the cross-sectional structure of the 2-in. test panel to observe three-dimensional IR emission used in this study. The panel specifications of the 2-in. test panel in Fig. 3 were exactly the same with the 42-in. panel specifications in Fig. 2 and Table 1, except for the phosphor layer. In Fig. 3, to observe the side view of the plasma discharge in a unit cell, one flank of the closed wall was replaced by a polished glass prism, which was made of fused silica. The side images reflected by the glass prism were measured together with the top images [9].

Fig. 4 shows the applied sustain driving waveform for the panel-aging process used in this study. The duty ratio and frequency for the sustain period was 40% and 25 kHz, respectively. The panel-aging process time was 3 h. The different sustain voltage levels of driving waveforms were applied to the test panel during the aging process, as listed in Table 2.

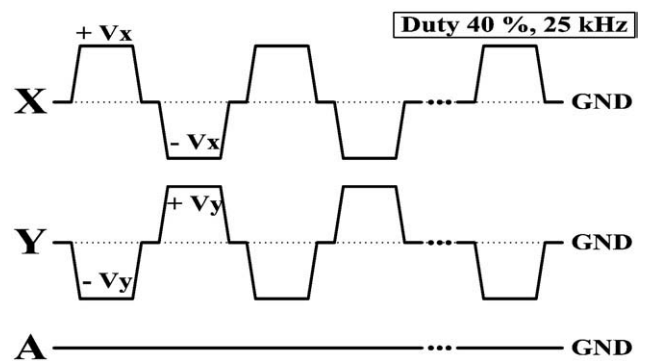


Fig. 4. Schematic diagram of sustain driving waveform for panel-aging process used in this study.

Table 1 Specifications of 42-in. and 2-in. AC-PDP used in this study.

Front Panel		Rear Panel	
ITO width	225 μm	Barrier rib width	55 μm
ITO gap	85 μm	Barrier rib height	120 μm
Bus width	50 μm	Address width	95 μm
Pixel pitch	912 \times 693 μm		
Gas chemistry	Ne–Xe (11%)–He (35%)		
Barrier rib type	Closed rib		

Table 2 Different voltage levels applied to test panels during aging process.

	+Vx, +Vy	–Vx, –Vy
Case 1	120 V	–120 V
Case 2	150 V	–150 V
Case 3	180 V	–180 V

Table 3
Comparison of discharge state detected by human eyes after panel-aging process under various sustain voltages.

	Discharge state after aging process
Case 1 (120 V)	Stable
Case 2 (150 V)	Unstable
Case 3 (180 V)	Unstable

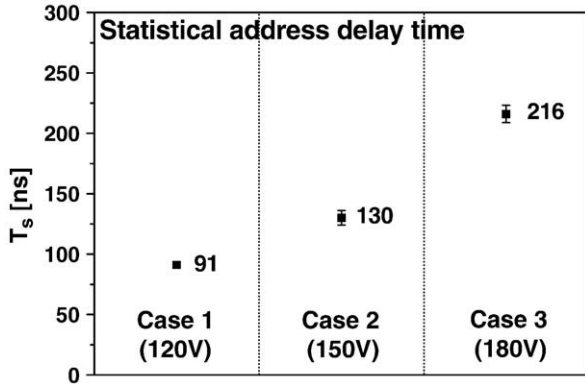


Fig. 5. Comparison of statistical address delay time during address period after panel-aging process under various sustain voltages.

3. Results and discussion

3.1. Experimental observation from 42-in. test panel

After the panel-aging process under the various sustain voltages, the discharge states are observed simply by the human eyes in Table 3, and the statistical address delay times (T_s) were measured in Fig. 5. As shown in Table 3, for case 1 (120 V), the stable discharge was produced after the panel-aging process. However, for cases 2 (150 V) and 3 (180 V), the unstable discharges were produced after the panel-aging process. Furthermore, for cases 2 and 3, i.e., higher sustain voltages, the statistical address delay times were observed to be delayed, as shown in Fig. 5.

To investigate the reason for the deteriorated discharge states after the panel-aging process under a higher sustain voltage, the SEM images were measured for the surface morphology of the MgO thin film positioned on the ITO and bus electrodes.

Fig. 6 shows the changes in the plane-SEM images of the MgO surfaces on the ITO and bus electrodes under the various sustain voltages in 42-in. test panels. As shown in Fig. 6, for case 1, the MgO surface morphologies for both ITO and bus electrodes were observed to be almost the same. However, for cases 2 and 3, i.e., higher sustain voltage cases, the MgO surface morphologies on the bus electrodes were observed to be larger than those on the ITO electrodes. We have reported that the continuous ion bombardment on the MgO thin film causes the surface morphology of the MgO thin film to get larger [6–8]. The surface morphologies shown in cases 2 and 3 of Fig. 6 mean that the MgO surface on the bus electrodes were more damaged compared

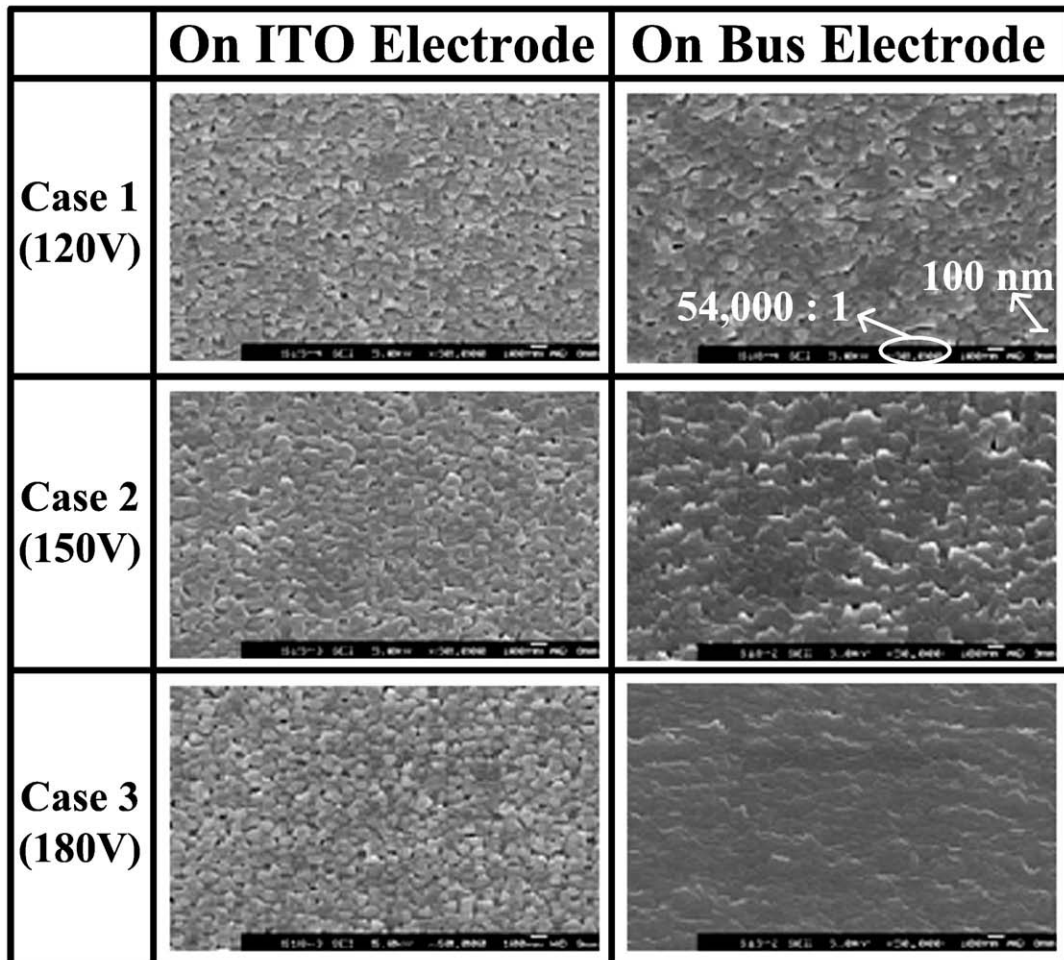


Fig. 6. Comparison of SEM images of MgO surface changes on ITO and bus electrodes after panel-aging process under various sustain voltages.

to those on the ITO electrodes. This result also implies that the severe ion bombardment has been made toward the bus electrode instead of the ITO electrode for the higher sustain voltage case. These experimental results showed that the unstable discharge condition after the panel-aging process under higher sustain voltage could be attributed to the difference of the MgO surface morphologies between on the ITO and bus electrodes.

3.2. Experimental observation of IR emission from 2-in. panel

To investigate the reason for the difference of the MgO surface morphologies between on the ITO and bus electrodes after the panel-aging process under a higher sustain voltage, the 2-in. test panel was

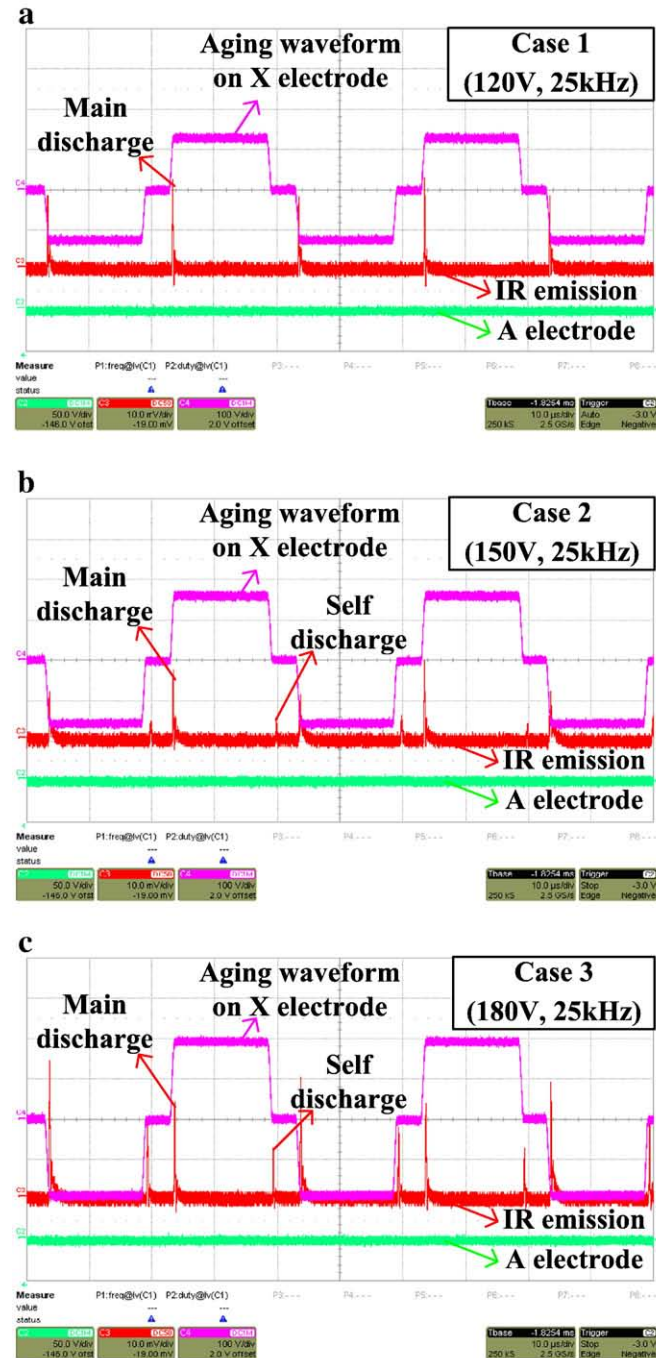


Fig. 7. Comparison of IR emissions during sustain period under various sustain voltages. (a) Case 1 = 120 V, (b) Case 2 = 150 V, and (c) Case 3 = 180 V.

fabricated to analyze the three-dimensional (3-D) spatiotemporal observations of the plasma discharge in PDP cell. The top and side discharge images were measured simultaneously by using the ICCD camera with the IR bandpass filter centered at 823 nm (10-nm bandwidth) [9].

Fig. 7 shows the changes in the IR emissions during the panel-aging discharge under the various sustain voltages. Unlike case 1, the weak IR peak was observed with the strong peak for cases 2 and 3, as shown in Fig. 7, which indicated that the weak IR peak emitted immediately after the falling of the sustain pulse was produced by the self-erasing discharge [10] during the panel-aging process.

Fig. 8 (a) shows the ICCD measurement points for measuring the two discharges, i.e., the main discharge after the rising of the sustain pulse and the self-erasing discharge after the falling of the sustain pulse. Fig. 8 (b) shows the time-integrated top and side ICCD images of the main and self-erasing discharges. As shown in Fig. 8 (b), for case 1, the self-erasing discharge during the panel-aging process was not observed. From the side view of case 1, the discharge intensities were observed to be almost the same for both ITO and bus electrodes. In this case, i.e., case 1, the MgO surface morphologies for both ITO and bus electrodes were observed to be almost the same, as shown in Fig. 6. However, for cases 2 and 3, the self-erasing discharge during the panel-aging process was observed. The side view data showed that for cases 2 and 3, the discharge intensities on the bus electrodes were stronger than those on the ITO electrodes, which was caused by the self-erasing discharges. In this case, i.e., cases 2 and 3, the MgO surface morphologies for both ITO and bus electrodes were observed to be quite different, as shown in Fig. 6.

The self-erasing discharge would alter the wall charge distributions accumulating on the ITO and bus electrodes. Even though the wall charges start to be erased near the ITO gap by the self-erasing discharge, parts of wall charges still remain on the bus electrodes. This altered wall charge distribution causes the ions to bombard toward the bus electrode instead of the ITO electrodes during the subsequent main discharge. The MgO surface on the bus electrode was more damaged due to the increase in the physical sputtering [6–8] induced by the severe ion bombardment, as confirmed by the result of Fig. 6. And also, for cases 2 and 3, according to the remains of the ions and electrons on the bus electrodes far away from the gap of ITO electrodes, the glow intensity on the cathode at the side view was very weak compared with those of anode and with that of case 1 due to the difference in the mobility of ions and electrons. However, for case 1, the discharge intensities on the cathode and anode were almost same due to the remains of the ions and electrons near gap of the ITO electrodes despite the difference in the mobility of ions and electrons.

3.3. Impulse of Xe, Ne ions near MgO surface along ITO and bus electrodes obtained from simulation

To identify the increase in the ion bombardment on the bus electrode caused by the self-erasing discharge during the panel-aging process, the 2-D fluid model of plasma [11] was used in this simulation.

Fig. 9 (a) shows the detection points of simulation results for detecting the wall charge distribution before applying the sustain pulse and the electric field strength after the rising of the sustain pulse. Fig. 9 (b) shows the wall charge distribution and electric field strength obtained from the simulation under various sustain voltages. As shown in Fig. 9 (b), for case 1, the electric field strengths were almost the same for both ITO and bus electrodes due to the same wall charge distribution on both the ITO and bus electrodes. However, for cases 2 and 3, i.e., higher sustain voltage cases, the electric field strengths on the bus electrodes were stronger than those on the ITO electrodes due to the erasing of the wall charges accumulated on the ITO electrode caused by the self-erasing discharges. This intensified

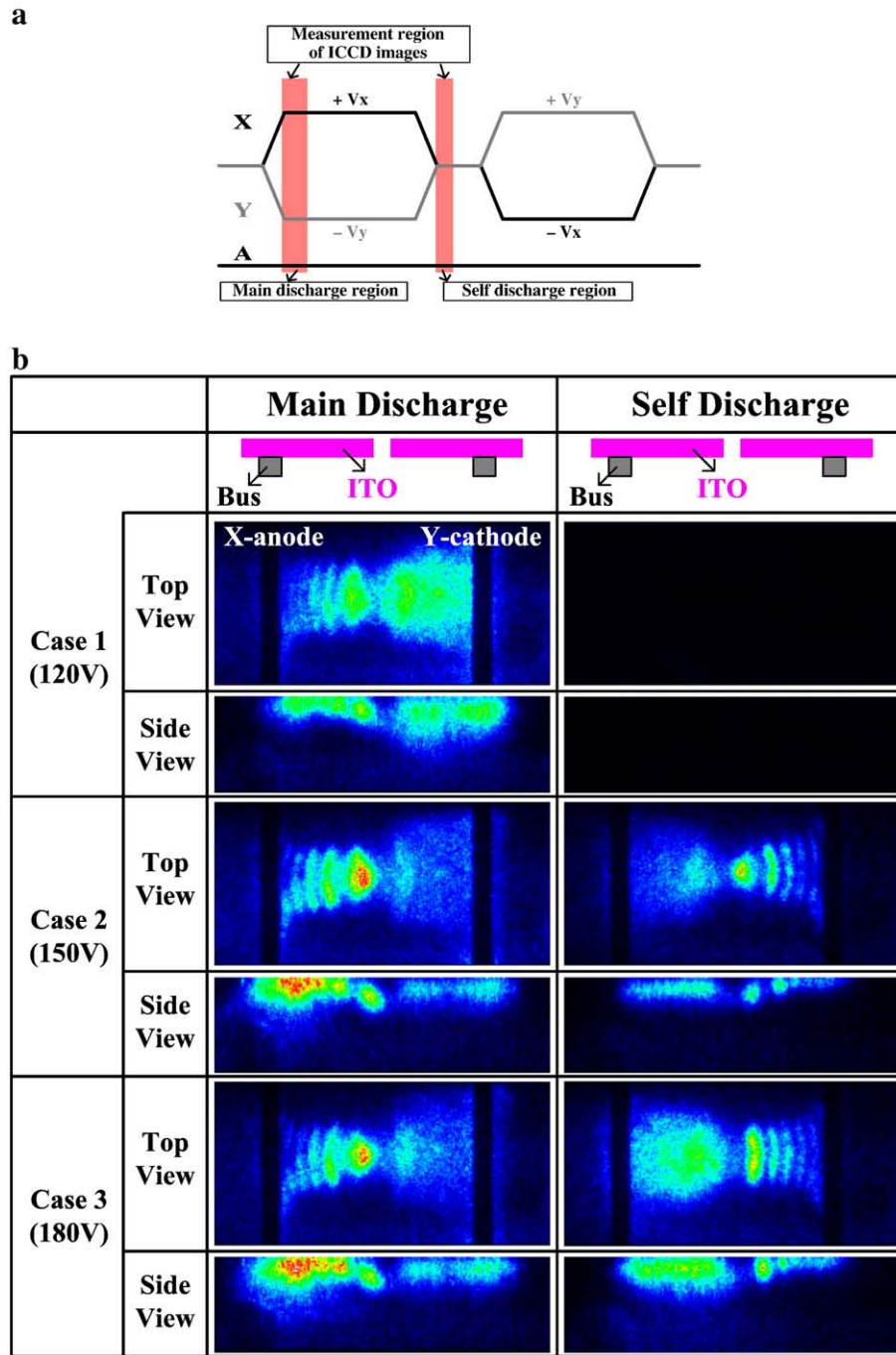


Fig. 8. (a) Schematic diagram of sustain driving waveform identical to waveform in Fig. 4 and measurement point of ICCD images, and (b) comparison of top and side ICCD images during sustain period under various sustain voltages.

electric field caused the ions to bombard severely toward the bus electrode instead of the ITO electrodes during the subsequent main discharge.

Fig. 10 shows the changes in the impulse of Xe and Ne ions near MgO surface along ITO and bus electrodes based on the simulation during the sustain discharge under the various sustain voltages. As shown in Fig. 10, for case 1, the impulse of Xe and Ne ions was almost the same for both ITO and bus electrodes. However, for cases 2 and 3, i.e., higher sustain voltage cases, the impulse of Xe and Ne ions on the bus electrodes was higher than those on the ITO electrodes. It means that the MgO surface on the bus electrodes was more damaged compared to those on the ITO electrodes due to the increase in the

impulse of Xe and Ne ions impinging on the MgO surface on the bus electrode. In this case, i.e., cases 2 and 3, the MgO surface morphologies for both ITO and bus electrodes were observed to be quite different, as confirmed by the result of Fig. 6.

4. Conclusion

In an AC-PDP manufacturing, the aging process is necessary to obtain a stable discharge. The aging process time and the reliability of an AC-PDP are related to the surface properties of the MgO thin film on the ITO and bus electrodes, which are mainly affected by the self-erasing discharge during the panel-aging process. The self-erasing

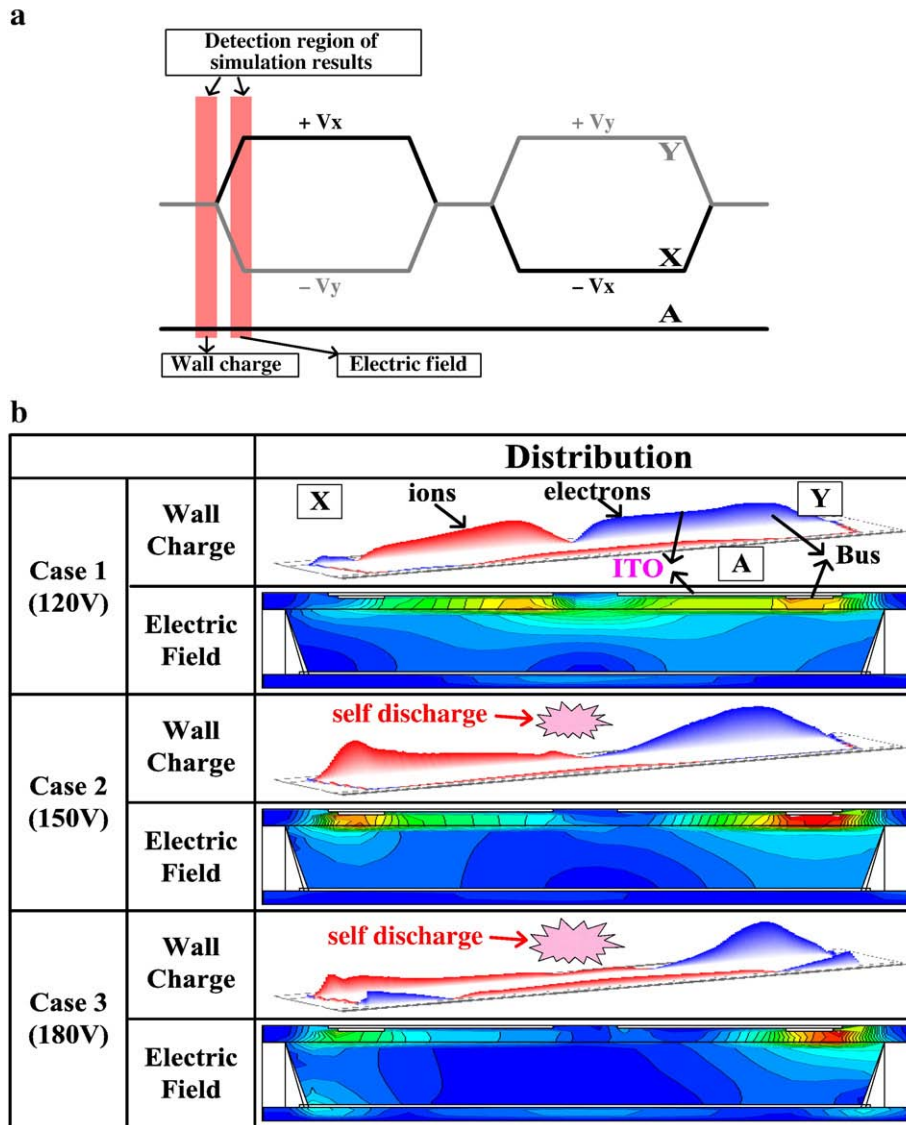


Fig. 9. (a) Schematic diagram of sustain driving waveform identical to waveform in Fig. 4 and detection point of wall charge and electric field and (b) comparison of wall charge and electric field based on simulated results during sustain period under various sustain voltages.

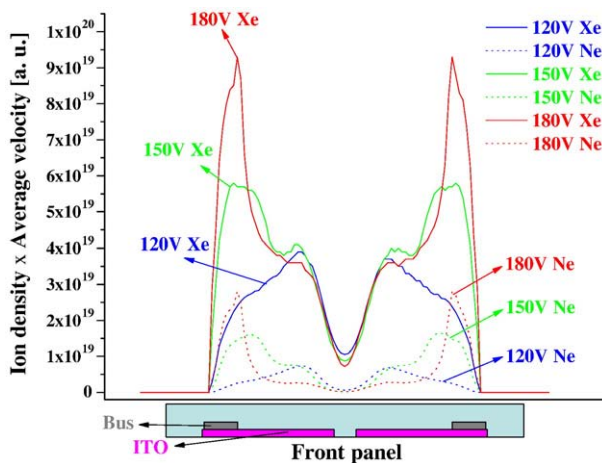


Fig. 10. Comparison of impulse of Xe and Ne ions near MgO surface along ITO and bus electrodes based on simulated results during sustain period under various sustain voltages, where impulse means ion density multiplied by average velocity.

discharge during the panel-aging process can induce the difference of the impulse of Xe and Ne ions impinging on the MgO surface on the ITO and bus electrodes due to the erasing of the wall charges accumulated on the ITO electrode caused by the self-erasing discharges. As a result, the self-erasing discharge during the panel-aging process hinders the stable sustain discharge because it is not effective to obtain the uniform surface morphology of the MgO thin film on the ITO and bus electrodes.

Acknowledgment

This work was supported in part by the IT R&D program of MKE/KEIT and in part by the Brain Korea 21 (BK21).

References

- [1] K.C. Choi, H.-J. Kim, B.J. Shin, IEEE Trans. Electron Devices 51 (2004) 1241.
- [2] M.S. Park, D.H. Park, B.H. Kim, B.G. Ryu, S.T. Kim, G.-W. Seo, D.-Y. Kim, S.-T. Park, J.-B. Kim, IMID/IDMC'06 Dig, 2006, p. 126.
- [3] K.-H. Park, M.-S. Ko, S.-H. Yoon, Y.-S. Kim, IMID'07 Dig, 2007, p. 216.
- [4] M. Noh, Y. Yi, K. Jeong, J. Korean Phys. Soc. 42 (2003) 631.

- [5] S.-K. Kwon, J.-H. Kim, S.-K. Moon, J.-K. Choi, Y.-I. Jang, K.-H. Park, S.-S. Han, *SID'09 Dig*, 2009, p. 359.
- [6] C.-S. Park, H.-S. Tae, Y.-K. Kwon, E.G. Heo, *IEEE Trans. Plasma Sci.* 35 (2007) 1511.
- [7] C.-S. Park, H.-S. Tae, Y.-K. Kwon, E.G. Heo, *IEEE Trans. Electron Devices* 54 (2007) 1315.
- [8] C.-S. Park, H.-S. Tae, *Appl. Opt.* 48 (2009) F78.
- [9] T.-S. Cho, J.-W. Jung, *IEEE Trans. Plasma Science* 37 (2009) 135.
- [10] H.-S. Tae, B.-G. Cho, S.-I. Chien, *IEEE Trans. Electron Devices* 50 (2003) 522.
- [11] S.-B. Song, P.-Y. Park, H.-Y. Lee, J.H. Seo, K.D. Kang, *Surf. Coating Technol.* 171 (2003) 140.